Glycobiology vol. 17 no. 12 pp. 1344–1356, 2007
doi:10.1093/glycob/cwm100
Advance Access publication on September 20, 2007

Ovarian cancer is associated with changes in glycosylation in both acute-phase proteins and IgG

Radka Saldova[2,4], Louise Royle[2,4], Catherine M Radcliffe[2,4], Umi M Abd Hamid[4], Rachel Evans[4], James N Arnold[3,4], Rosamonde E Banks[5], Richard Hutson[6], David J Harvey[4], Robin Antrobus[4], Stefana M Petrescu[7], Raymond A Dwek[4], and Pauline M Rudd[1,2,4]

[4]Department of Biochemistry, Oxford Glycobiology Institute, University of Oxford, Oxford OX1 3QU, UK; [5]Cancer Research UK Clinical Centre, and [6]Department of Obstetrics and Gynaecology, St James's University Hospital, Leeds LS9 7TF, UK; and [7]Institute of Biochemistry, Splaiul Independentei 296, 060031 Bucharest 17, Romania

Received on May 28, 2007; revised on August 20, 2007; accepted on September 9, 2007

Ovarian cancer is the fourth most common cancer in women in the Western world. In a pilot scale study, we highlight changes in the total serum glycome of patients with advanced ovarian cancer that might shed insight into disease pathogenesis. These changes include increases in levels of core fucosylated, agalactosyl biantennary glycans (FA2) and sialyl Lewis x (SLe^x). To investigate further which proteins contribute to these alterations, we developed technology to analyze simultaneously the glycosylation of protein glycoforms contained in single spots excised from a 2D gel (<1 ng protein). The acute-phase proteins, haptoglobin, α1-acid glycoprotein, and α1-antichymotrypsin from patients contained elevated levels of subsets of glycoforms containing SLe^x. We also established that IgG heavy chains from patients contained twice the level of FA2 compared with healthy controls. Serum CA125 is the only biomarker that is used routinely, and there is a need for complementary markers that will improve both sensitivity and specificity. There was some preliminary indication that combinations of changes in the serum glycome might improve the separation of ovarian cancer and benign tumors; however, a larger study using data receiver operating characteristic curves will be required to draw any firm conclusions.

Keywords: acute-phase proteins/biomarker/IgG/*N*-linked glycans/ovarian cancer

Introduction

Ovarian cancer is the most lethal of all gynecological cancers among women according to UK cancer mortality statistics (Cancer Research, UK; http://info.cancerresearchuk.org/cancerstats/mortality/cancerdeaths/). Most patients are diagnosed when the disease is in an advanced stage (Duffy et al. 2005). The earlier the cancer is diagnosed, the higher is the 5-year survival rate, which is more than 90% for early stage, but in advanced stages III and IV decreases to 30% (Duffy et al. 2005). Currently, ovarian cancer is most frequently diagnosed by ultrasonography and the serum marker CA125 (Duffy et al. 2005). CA125 is currently the best marker for ovarian cancer, but is not reliable for diagnosing early-stage cancers (Duffy et al. 2005). CA125 is elevated in 80–90% of ovarian cancer patients; the level rising with the stage of the disease. In addition, it is also higher in nonmucinous tumors than in mucinous ones (Duffy et al. 2005). CA125 can give a false positive response in benign conditions, pregnant women, and other cancers (Duffy et al. 2005). Essentially, this illustrates that additional markers are needed for the diagnosis of this lethal cancer which would complement the use of CA125.

Several potential markers are currently being investigated including OVX1, M-CSF, inhibin, kallikreins, TPS, and lysophosphatidic acid (Bast et al. 2005; Duffy et al. 2005). Increasingly, proteomics-based approaches in several studies illustrate the potential for ovarian cancer biomarkers (Ahmed et al. 2005; Kozak et al. 2005; Ye et al. 2006; Bengtsson et al. 2007).

In human carcinomas, changes in glycosylation have been described including the presence of sialyl Lewis x (SLe^x) (Magnani 2004; Tabares et al. 2006). The SLe^x epitope consists of a GlcNAc residue with an α1,3-linked fucose as well as a β1,4-linked galactose which has an α2,3-linked sialic acid (Table I, peak id 12). SLe^x is a selectin ligand (binding to E-selectin, P-selectin, and L-selectin) and has been proposed to be involved in tumor metastasis (McEver 1997). SLe^x has also been shown to be upregulated during chronic inflammation on haptoglobin, α1-acid glycoprotein, and α1-antichymotrypsin (Brinkman-van der Linden et al. 1998) and in neutrophils (Fukuda et al. 1984). Previous reports in ovarian cancer have indicated that there is a change of glycosylation on haptoglobin (Turner et al. 1995) and IgG (Gercel-Taylor et al. 2001) in ovarian cancer patients.

The aim of this study was to identify which proteins were contributing to changes in the serum glycome of ovarian cancer patients, and to determine whether changes in glycans of serum proteins could have potential utility as markers in ovarian cancer. In an initial pilot study analyzing the total serum *N*-glycans using quantitative and detailed normal phase (NP) high-performance liquid chromatography (HPLC), weak anion exchange (WAX) HPLC, and mass spectrometry (MS), samples from three patients with advanced ovarian cancer were compared to a pooled control sample. Based on the findings, we subsequently used our recently developed high-throughput technology to monitor SLe^x and FA2 (core fucosylated agalactosylated biantennary glycan structure) levels

[1]To whom correspondence should be addressed: Tel: +353-17166728; Fax: +353-17166950; e-mail: pauline.rudd@nibrt.ie
[2]Present address: Dublin-Oxford Glycobiology Laboratory, NIBRT, Conway Institute, University College of Dublin, Belfield, Dublin 4, Ireland
[3]Present address: National Heart and Lung Institute, Imperial College London SW3 6LR, UK

Table I. Summary of the glycans identified as altered in ovarian cancer patients

	Fraction			Neutral			Monosialylated
[1]Peak ID	1	2	3	4	5	6	7
[2]Structure	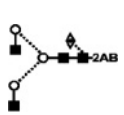	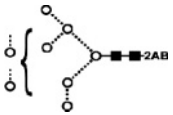	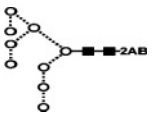	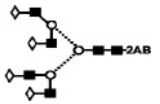	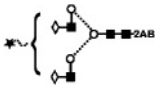	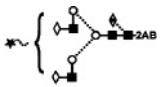	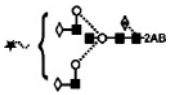
Abbreviation	FA2	M8	M9	A4G4	A2G2S1	FA2G2S1	FA2BG2S1
[3]MS	Hex3HexNAc4 Fuc1	Hex8HexNAc2	Hex9HexNAc2	Hex7HexNAc6	Hex5HexNAc4 NeuNAc1	Hex5HexNAc4 Fuc1NeuNAc1	Hex5HexNAc5 Fuc1NeuNAc1
GU	5.82	8.89		9.49	8.08	8.46	8.63
Patient A	27.7	3.2		9.7	39.6	10.5	8.2
Patient B	20.9	3.8		7.0	48.5	15.0	8.1
Patient C	32.4	4.1		8.4	40.2	16.0	11.0
Patient average	27.0 ± 4.7	3.7 ± 0.4		8.4 ± 1.1	42.8 ± 4.1	13.8 ± 2.4	9.1 ± 1.4
Control Glycoprotein	10.8 IgG	5.7		6.1	34.4	18.0	16.4

Fraction	Disialylated			Trisialylated		Whole serum	
Peak ID	8	9	10	11	12	1	12
[2]Structure	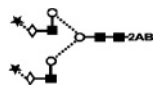	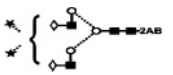	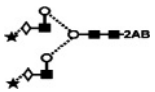	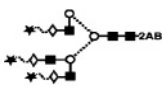		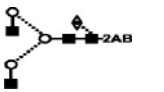	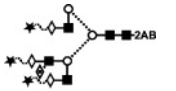
Abbreviation	[4]A2G2S(6,6)2	[4]A2G2S(3,6)2	[4]A2G2S(3,3)2	A3G3S3	[6]A3F1G3S3	FA2	[6]A3F1G3S3
[3]MS	Hex5HexNAc4 NeuNAc2	Hex5HexNAc4 NeuNAc2	Hex5HexNAc4 NeuNAc2	Hex6HexNAc5 NeuNAc3	Hex6HexNAc5 Fuc1NeuNAc3	Hex3HexNAc4 Fuc1	Hex6HexNAc5 Fuc1NeuNAc3
GU	8.86	8.86	8.86	10.00	10.50	5.82	10.50
Patient A	64.0	33.8	2.2	12.3	65.3	2.9	17.7
Patient B	61.5	35.7	2.8	24.8	58.3	2.7	13.8
Patient C	61.1	36.0	2.9	33.7	57.6	4.5	12.9
Patient average	62.2 ± 1.3	35.2 ± 1.0	2.6 ± 0.3	23.6 ± 8.8	60.4 ± 3.5	3.4 ± 0.8	14.8 ± 2.1
Control Glycoprotein	59.0	37.6	3.4	39.6 [5]HP,AGP,ACH	46.1	1.9 IgG	6.5 [5]HP, AGP, ACH

[1] Peak ID relates to Figure 1.
[2] Structure abbreviations: all *N*-glycans have two core GlcNAcs; F at the start of the abbreviation indicates a core fucose α1–6 to inner GlcNAc; Man (x), number (x) of mannose on core GlcNAcs; A(x), number (x) of antenna (GlcNAc) on trimannosyl core; B, bisecting GlcNAc linked β1–4 to β1–3 mannose; F(x), number (x) of fucose linked α1–3 to antenna GlcNAc, G(x), number (x) of galactose on antenna; S(x), number of sialic acids on antenna. All structures were confirmed by exoglycosidase sequencing and also by MALDI MS from composition as $[M+Na]^+$ ions, all masses within 0.2 Da of calculated.
Symbol representation of glycans in as follows: GlcNAc, filled square; mannose, open circle; galactose, open diamond; fucose, diamond with a dot inside; beta linkage, solid line; alpha linkage, dotted line; 1–4 linkage, horizontal line; 1–3 linkage, (/); 1–2 linkage, vertical line; and 1–6 linkage, (\).
[3] ID by MALDI and ESI MS/MS fragmentation.
[4] Identified by digestion by α2–3 specific sialidase NAN1.
[5] HP, haptoglobin β-chain; AGP, α1-acid glycoprotein; ACH, α1-antichymotrypsin.
[6] Contains a SLe^x epitope.

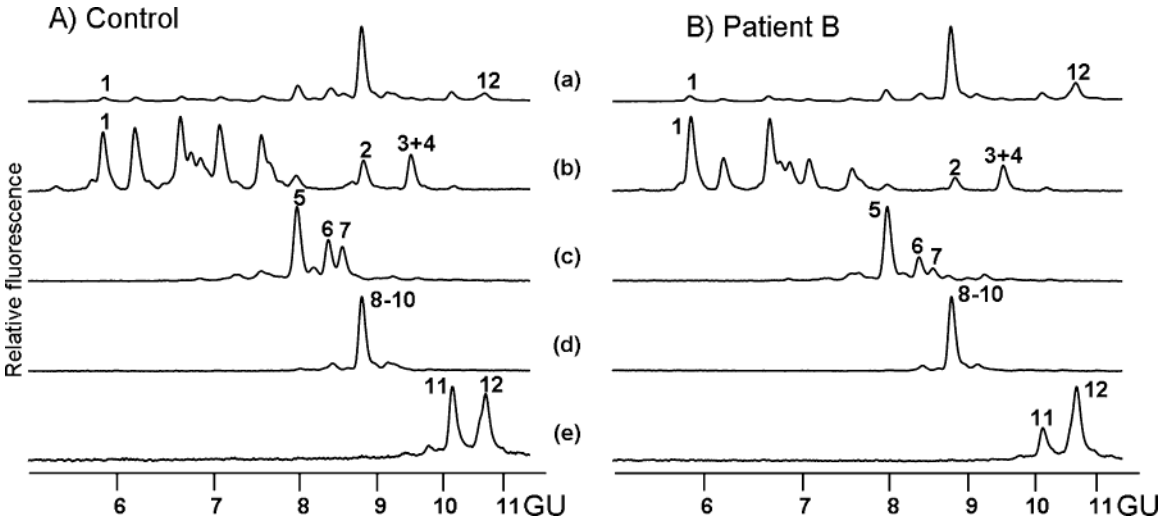

Fig. 1. Typical NPHPLC chromatograms of glycans previously separated by charge on WAXHPLC from (**A**) control sample and (**B**) stage III ovarian cancer patient samples. (a) whole unfractionated serum glycans, (b) neutral fraction, (c) monosialylated fraction, (d) disialylated fraction, (e) trisialylated fraction. See Table I for peak ID. All structures in each peak have been fully characterized previously by Royle et al. (2006). The peaks numbered above correspond to those which were consistently different from controls in all three patients.

in a total of 90 samples from healthy controls, patients with ovarian cancer, benign gynecological conditions or other gynecological cancers. This confirmed the initial findings of increased expression in patients with ovarian cancer compared with controls or benign conditions and also in other cancers. Further preliminary investigations using our newly developed highly sensitive techniques to determine the glycosylation status of proteins isolated from individual spots on fluorescently stained 2D-sodium dodecyl sulphate (SDS)-polyacrylamide gel electrophoresis (PAGE) gels found major and variable differences in glycoforms of several acute-phase proteins including haptoglobin, α1-acid glycoprotein, α1-antichymotrypsin, and also in IgG.

Results

Identification of N*-glycosylation changes in serum ovarian cancer patients*

The *N*-glycans were identified using quantitative NPHPLC and exoglycosidase digestion with structural assignments made using database matching (GlycoBase; http://glycobase.ucd.ie/cgi-bin/public/glycobase.cgi) combined with matrix-assisted laser desorption/ionization time-of-flight (MALDI-TOF) and negative ion nanoelectrospray mass spectrometric analysis, as described previously (Harvey 2005a, 2005b, 2005c; Royle et al. 2006). The *N*-linked glycosylation changes in three ovarian cancer patients were analyzed in a preliminary study to identify specific glycan structures, the levels of which were altered in the patient samples. The results from these sera were compared to those from a healthy control pool (five normal sex- and age-matched serum samples).

Whole serum glycans from three patients were fractionated on WAXHPLC according to charge and each fraction was subsequently analyzed by NPHPLC, represented by the profiles from a stage III ovarian cancer patient (B) and the control sample (Figure 1). The relative amounts of sialylated glycans were calculated from WAXHPLC (Table II). From these data the levels of monosialylated glycans from the patient samples were about half that of the control pool while there were increased (approximately double) levels of the tri- and tetrasialylated glycans. There was no trend in the change in relative amounts of disialylated glycans. Glycan structures in the fractions were confirmed using exoglycosidase digestions, NPHPLC, and MALDI MS. Percentage areas of each glycan from the WAX fractions and in whole serum are shown in Table I which summarizes the glycans identified in NPHPLC chromatograms of the WAX fractions and the levels of them.

In the *neutral* fractions of the serum *N*-linked glycans: the core fucosylated biantennary glycan (FA2) is increased from 10.8 to 27.0 (±4.7)% in patients; $Man_8GlcNAc_2$ (M8) is decreased from 5.7 to 3.7 (±0.4)% in cancer; whereas the peak containing both $Man_9GlcNAc_2$ (M9) and the tetragalactosylated

Table II. Relative% areas of charged glycans from WAXHPLC

Sample	Monosialylated	Disialylated	Trisialylated	Tetrasialylated
Patient A	13.0	58.3	25.1	3.5
Patient B	13.5	56.2	23.9	6.4
Patient C	14.8	56.9	24.0	4.3
Patient average	13.8	57.1	24.3	4.7
Standard deviation	0.77	0.91	0.55	1.22
Patient average	13.8 ± 0.8	57.1 ± 0.9	24.3 ± 0.6	4.7 ± 1.2
Control	24.6	58.1	14.3	3.1

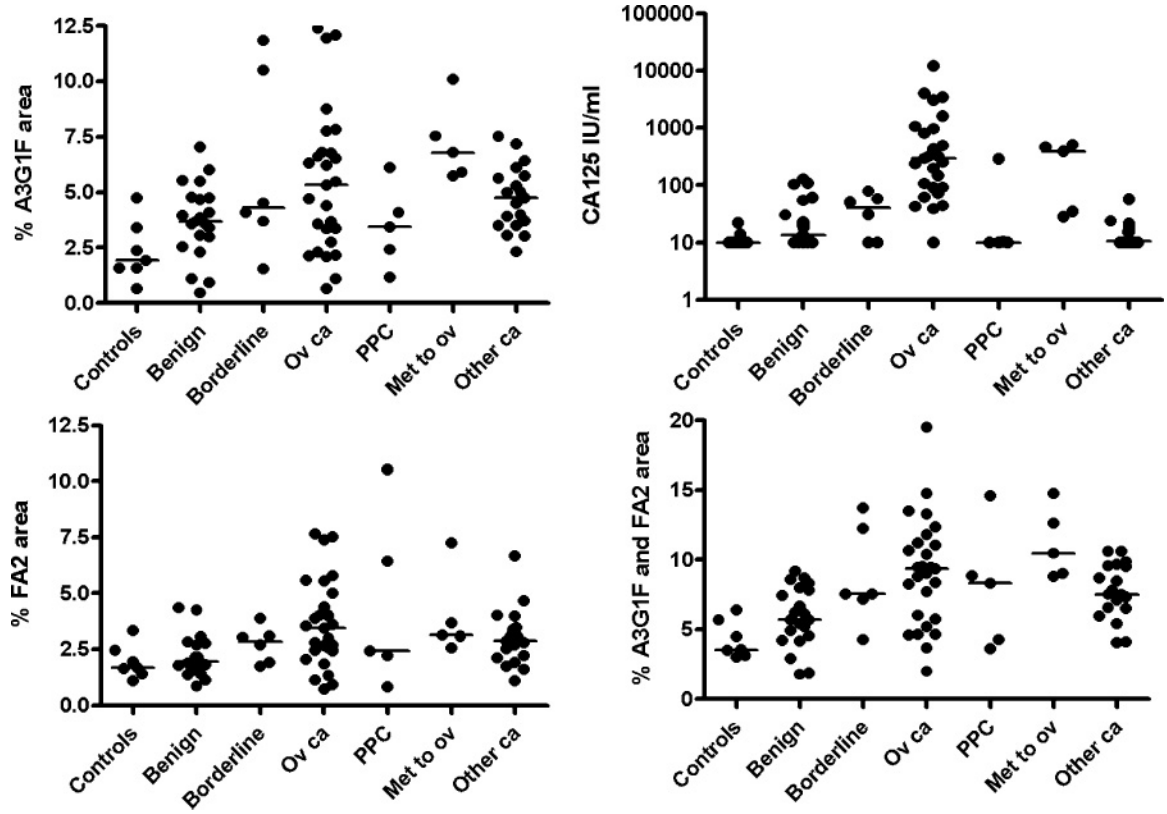

Fig. 2. Comparison of SLe^x (A3G1F), FA2, A3F1G1 together with FA2 and CA125 levels in Leeds serum samples (healthy controls, benign gynecological conditions, borderline ovarian tumors, ovarian cancer (ov ca), primary peritoneal carcinomatosis (PPC), endometrial cancer metastasized to ovary (met to ov) and other gynecological cancers).

tetra-antennary structure (A4G4) is increased from 6.1 to 8.4 (±1.1)%.

In the *monosialylated N*-linked glycan fractions, there is a decrease in fucosylation in the cancer samples. The core fucosylated digalactosylated monosialylated structures with and without bisects (B), FA2G2S1 and FA2BG2S1, are reduced from 18.0 to 13.8 (±2.4)% (and 16.4 to 9.1 (±1.4)%, respectively), while the digalactosylated monosialylated structures (A2G2S1) are increased from 34.4 to 42.8 (±4.1)% in the stage III.

In the *disialylated* fractions, the amount of α2,3 sialic acid levels were only slightly lower compared to α2,6 sialic acid levels in the three patients studied (stage III ovarian cancer) than in the control. In Table I, it is shown that A2G2S(6,6)2 is increased from 59.0 to 62.2 (±1.3)% but A2G2S(3,6)2 is decreased from 37.6 to 35.2 (±1.0)% and A2G2S(3,3)2 is decreased from 3.4 to 2.6 (±0.3)%. These structures were confirmed by *Streptococcus pneumoniae* sialidase (NAN1) which digests only α2,3 links.

The *trisialylated* fractions showed increased outer arm fucosylation in cancer. A SLe^x containing the triantennary glycan (A3F1G3S3) is increased from 46.1 to 60.4 (±3.5)% whereas the trisialylated nonfucosylated glycan (A3G3S3) is decreased from 39.6 to 23.6 (±8.8)% in stage III ovarian cancer.

Overall, the most striking differences between the cancer serum glycans and those from healthy controls, which are also observed clearly in the unfractionated whole serum glycan pool, are the doubling in the levels of A3F1G3S3 (increase from 6.5 to 14.8 (±2.1)%) and FA2 (increase from 1.9 to 3.4 (±0.8)%).

We carried out a more extensive study into the levels of SLe^x, FA2 and CA125 in 90 serum samples from healthy controls, patients with benign gynecological conditions, borderline ovarian tumors, ovarian cancer, primary peritoneal carcinomatosis, endometrial cancer metastasized to the ovary and other gynecological cancers (Figure 2). The released glycans were digested with sialidase and β1-4 galactosidase to give the structure A3F1G1. This digestion segregates the SLe^x containing structures from coeluting glycans that are digested to lower glucose unit (GU) value peaks, leaving a clearly separated peak for integration to give an accurate percentage of total glycans.

The analysis of SLe^x clearly shows significantly elevated levels in patients with ovarian cancer compared with healthy controls ($p = 0.01$), although the number of control samples is small ($n = 7$) and covers a slightly younger age range (see Table III). However, the difference between patients with other cancers or cancers which had metastasized to the ovary compared with controls was more marked ($p = 0.002$). Additionally the patients with benign gynecological conditions also showed levels which overlapped considerably and were not significantly different from those of the cancer patients. This contrasts markedly with the CA125 results, which show much better specificity for the ovarian cancer group.

The analysis of FA2 clearly shows significantly elevated levels in patients with ovarian cancer compared with healthy controls ($p = 0.022$) and with benign gynecological conditions ($p = 0.0054$). The difference between patients with ovarian cancer and other gynecological cancers was not significant.

Table III. Details of the female patient samples used in the main part of the study for determination of FA2 and SLe^x

	Number	Median age (range)
Healthy controls	7	55 (43–61)
Benign gynecological conditions (principally endometriosis or cysts)	21	44 (36–74)
Borderline ovarian tumors	6	67 (37–80)
Ovarian cancer (21 at presentation, six at relapse with advanced disease; 16 serous, 11 mucinous, endometrioid or clear cell; all FIGO stages)	27	58 (39–84)
Primary peritoneal carcinomatosis	5	67 (56–70)
Endometrial cancer metastasized to ovary (four carcinoma, one sarcoma)	5	72 (43–90)
Other gynecological cancers (16 endometrial carcinoma, two cervix, one fallopian tube)	19	67 (53–81)

Analysis of FA2 combined with SLe^x clearly shows more significantly elevated levels in patients with ovarian cancer compared with healthy controls ($p = 0.0016$) and compared with benign gynecological conditions ($p = 0.0016$). However, the difference between patients with ovarian cancer and other gynecological cancers was not significant. This suggests that a combination of these two markers would improve the diagnosis of ovarian cancer. This would need to be formally analyzed using larger groups of patients with receiver operating characteristic curves.

The possibility that the changes in SLe^x reflect underlying inflammatory changes was examined by a comparison with C-reactive protein (CRP) concentrations for all samples where a positive correlation was found ($p = 0.0023$; $r = 0.32$; CI = 0.12–0.5). When all the individual groups were examined, the "other cancer" group also showed a significant correlation between CRP and SLe^x levels ($p = 0.029$, $r = 0.500$, CI = 0.0445–0.783). It was however apparent that several patients showed marked acute-phase response but not elevated SLe^x levels and the converse was also true. The only other group where a significant correlation between CRP and SLe^x levels was found was the combined group of ovarian cancer and primary peritoneal carcinomatosis (PPC) ($p = 0.0025$, $r = 0.516$, CI = 0.193–0.738).

The correlation between CRP and CA125 was higher ($p < 0.0001$; $r = 0.41$; CI = 0.22–0.57) than between CRP and SLe^x in all samples taken together. When all the individual groups were examined, the only significant correlation between CRP and CA125 was found for the combined ovarian cancer and PPC group ($p = 0.0009$, $r = 0.559$, CI = 0.251–0.764). Correlation between CRP and FA2 was not significant overall or in individual groups.

Interestingly, we found no change in glycosylation of serum glycans in malignant melanoma samples compared to benign samples and controls, where inflammation is not involved (preliminary data, Figure 3). For all patients, the fibrinogen level was determined and the concentrations varied between 280 and 370 ng/mL. Normal values for this protein which increases in inflammation are 200–400 ng/mL. This confirms that these melanoma patients have a low level of inflammatory processes.

Identification of glycoproteins occupied by the target glycans

Having identified specific changes in glycan structures from whole serum glycoproteins, the next aim was to carry out some initial studies to identify which individual glycoproteins carried these glycans. A doubling in the level of FA2 glycan was found: this structure has previously been shown to be on immunoglobulin G (IgG) (Parekh et al. 1985). We therefore isolated IgG by affinity chromatography on a Protein G column and analyzed the *N*-linked glycans from the heavy chain (Figure 4 and Table IV). IgG containing agalactosylated structures (G0) (mostly represented by FA2) were doubled (increased from 27.1 to 53.2 (±3.3)%); monogalactosylated (G1) decreased (from 33.2 to 27.1 (±5.3)%); digalactosylated (G2) structures decreased (from 22.3 to 8.5 (±1.9)%); the overall sialylation decreased (from 17.5 to 11.2 (±6.6)%) (Table IV). All structures were confirmed by exoglycosidase digestions (Parekh et al. 1985).

Haptoglobin β-chain has previously been shown to be aberrantly glycosylated in cancer (Thompson and Turner 1987). Therefore, we examined the serum proteome to see if these and other glycoproteins showed glycosylation changes. 2D SDS-PAGE was employed to separate the ovarian cancer serum

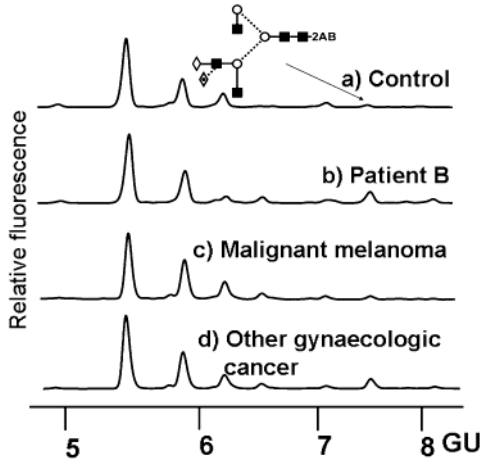

Fig. 3. Typical NPHPLC chromatograms of serum glycans after sialidase and β1–4 galactosidase digestion from (**a**) control sample, (**b**) stage III ovarian cancer patient, (**c**) malignant melanoma, (**d**) other gynecological cancer.

Table IV. Glycans from IgG heavy chain isolated by SDS-PAGE

Sample	G0	G1	G2	S
Patient A	50.5	25.0	9.7	14.9
Patient B	57.8	34.4	5.8	2.0
Patient C	51.4	21.8	10.0	16.8
Patient average	53.2	27.1	8.5	11.2
Standard deviation	3.25	5.34	1.90	6.56
Patient average	53.2 ± 3.3	27.1 ± 5.3	8.5 ± 1.9	11.2 ± 6.6
Control	27.1	33.2	22.3	17.5

NPHPLC percentage areas of neutral glycans (G0 = no galactose; G1 = 1 galactose; G2 = 2 galactoses) and sialylated glycans.

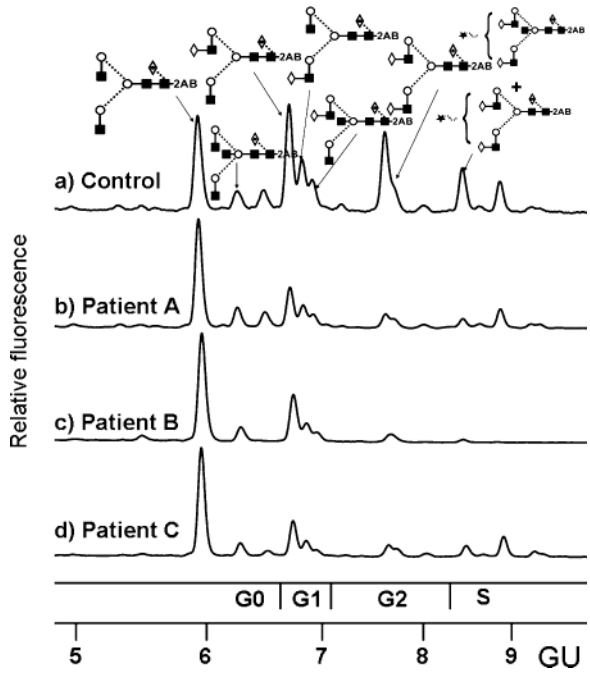

Fig. 4. NPHPLC chromatograms of serum glycans released from IgG heavy chain purified by SDS-PAGE. (**a**) control sample and (**b**)–(**d**) stage III ovarian cancer patient samples:. G0 – agalactosylated, G1 – monogalactosylated, G2 – digalactosylated, S – sialylated glycan structures.

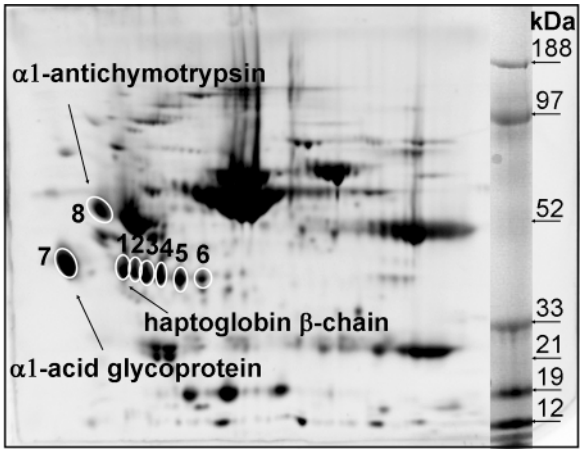

Fig. 5. Serum proteins from patient B (stage III ovarian cancer) were separated by 2-DE using 7 cm pH 3–10 nonlinear immobilized pH gradients (pH 3–10 NL IPG) and 4–12% SDS-PAGE gradient gels. Gels were stained using a fluorescent dye (OGT 1238), and the images were captured using Fuji LAS-1000 Camera.

proteins, and then these protein spots were cut out and screened for possible altered glycosylation by glycan analysis of each individual spot.

Figure 5 shows 2D electrophoresis of total serum from a stage III ovarian cancer patient B. *N*-glycans were released from these individual spots which were identified using mass spectrometric analysis (Table V) to be haptoglobin β-chain glycoforms (He et al. 2006), α1-acid glycoprotein, and α1-antichymotrypsin. In the cases of haptoglobin β-chain, α1-acid glycoprotein, and α1-antichymotrypsin, we found major glycosylation changes (Figures 6 and 7). Haptoglobin was identified in the train of spots 1–6 with the highest protein score, except for complement C3 in spot 1 (Table V). However, the *N*-linked glycosylation of complement C3 is known to consist of mannose structures (Crispin et al. 2004), so the complex glycans detected over all these spots originated from haptoglobin, although traces of mannose have been detected too reflecting the comigration of C3. α1-Antichymotrypsin was identified in spot 8 with the highest protein score, although α1-antitrypsin was also found in this spot, but identified with lower score (Table V) and with no glycans highlighted on α1-antichymotrypsin (unpublished data); therefore, it also does not interfere with altered levels of glycans described on α1-antichymotrypsin (Figure 7).

Figure 6 shows the NPHPLC profiles of haptoglobin β-chain glycoforms from single spots in the train on 2D minigels of a control and stage III ovarian cancer patient B; Figure 7 shows NPHPLC profiles of α1-acid glycoprotein 2D gel spots from pooled control, benign, malignant, and metastatic sera and α1-antichymotrypsin from pooled malignant samples cut from a single 2D gel spot digested by exoglycosidases for structural assignment of the outer arm fucosylated structures.

We identified the A3F1G3S3 on haptoglobin β-chain, α1-acid glycoprotein, and α1-antichymotrypsin. These changes in the relative proportions of glycoforms in the ovarian cancer patients' proteins contribute to the changes in the glycan profiles of whole serum, in particular to the neutral and trisialylated fraction of WAXHPLC.

Similar profile changes were observed in all six haptoglobin β-chain spots and in an advanced ovarian cancer patient (Figure 6), and pooled ovarian cancer patients sera comparing malignant and metastatic sera to benign and control sera (unpublished data). We have demonstrated that the different spots contained different subsets of glycoforms. With increased acidity, the glycoform migrated further to the left on the gel (Figure 5). In haptoglobin β-chain, the level of A3F1G3S3 is highest and A2G2S1 lowest in the most acidic glycoform (Figure 6).

Discussion

Changes in glycan structures in ovarian cancer serum samples

Several glycosylation changes in advanced ovarian cancer patients have been observed. The most significant were increased levels of SLe^x and FA2.

Increased levels of SLe^x in the trisialylated fraction suggest a change in the regulation of fucosyltransferases in the liver hepatocytes. To result in SLe^x structures, the precursor core structure has to be sialylated first and then fucosylated by α(1,3/1,4) fucosyltransferases (Aubert, Panicot-Dubois, et al. 2000; Magnani 2004). Increased levels of SLe^x have been correlated to decreased expression of α1,2 fucosyltransferase, which competes with α2,3 sialyltransferase for the same substrate (Aubert, Panicot, et al. 2000) and increased expression of α(1,3/1,4) fucosyltransferases in human pancreatic cancer cells (Aubert, Panicot-Dubois, 2000). We have determined the levels of SLe^x in different stages of ovarian and other gynecological cancers and compared them to benign gynecological conditions and demonstrated that, although higher than controls, they are not specific for ovarian cancer. We have also identified an increase in both branching and sialylation in whole serum *N*-glycans

Table V. Identification of protein spots from 2-DE (shown in Figure 5) by nanospray-quadrupole time-of-flight-MS/MS of tryptic peptides followed by MASCOT search of SWISS-PROT database

Gel spot	[1]Identification	Accession number	Protein covered (%)	Protein score	Number of peptides matched
1	Complement C3	P01024	13.0 ± 0.5	729.5 ± 170.7	17 ± 2
1	Haptoglobin β-chain	P00738	29.2 ± 0.6	421.7 ± 44.0	5 ± 4
1	Zinc-α2-glycoprotein	P25311	12.7 ± 5.3	88.6 ± 2.7	3 ± 1
1	Complement C4-A	P0C0L4	3.72	48.7	2
1	Serum paraoxogenase/ arylesterase 1	P27169	4.2	46.7	1
2	Haptoglobin β-chain	P00738	36.3 ± 1.1	532.2 ± 78.2	12 ± 2
2	Complement C3	P01024	1.7 ± 0.5	88.3 ± 37.7	2 ± 1
2	Serum paraoxogenase/ arylesterase 1	P27169	4.2	71.6 ± 0.5	1
2	Zinc-α2-glycoprotein	P25311	3.4	55.8	1
3	Haptoglobin β-chain	P00738	28.0 ± 2.6	501.6 ± 4.5	11 ± 1
3	Serum paraoxogenase/ arylesterase 1	P27169	4.2	59.9	1
4	Haptoglobin β-chain	P00738	37.0 ± 1.7	608.7 ± 40.8	14
4	Serum paraoxogenase/ arylesterase 1	P27169	4.2	63.9	1
5	Haptoglobin β-chain	P00738	28.9 ± 0.4	547.0 ± 111.1	14 ± 2
6	Haptoglobin β-chain	P00738	28.7 ± 3.8	458.4 ± 93.4	10 ± 2
7	α1-acid glycoprotein	P02763	9.0 ± 4.0	87.9 ± 22.7	3 ± 1
8	α1-antichymotrypsin	P01009	29.4 ± 13.2	571.2 ± 274.5	11 ± 5
8	α1-antitrypsin	P01011	16.6 ± 9.5	134.7 ± 78.9	4 ± 2
8	Kininogen-1	P01042	6.5 ± 3.6	121.5 ± 76.6	3 ± 2

[1]Only glycoproteins identified in spots listed (unglycosylated proteins not listed).

in three advanced ovarian cancer patients (Table II). Increased branching creates more sites for terminal sialic acid residues and together with sialyltransferase upregulation increases the sialylation (Kim and Varki 1997). This has been shown to correlate with advanced stage, tumor progression, and metastasis (Kim and Varki 1997). These changes reflect differences in expression levels of sialyltransferase and fucosyltranferases in the Golgi of the liver hepatocytes (Dube and Bertozzi 2005).

In addition to the increase in overall sialylation, we also found slightly lower levels of α2,3 sialic acid levels compared to α2,6 in the disialylated fractions. These findings are in agreement with previous findings of decreased mRNA expression of α2,3 sialyltransferases responsible for *N*-linked glycosylation and increased α2,6 sialyltransferase in tumor tissues of ovarian cancer patients (Wang et al. 2005).

Increased levels of SLe^x and branching of *N*-glycans have also been reported in chronic inflammation (De Graaf et al. 1993; Brinkman-van der Linden et al. 1998). As chronic inflammation is often observed in cancer (Llorca et al. 2007), these glycan changes may be associated with the inflammation and not just the cancer. However, these glycan measurements could still be very useful in cancer prognosis similarly to CRP

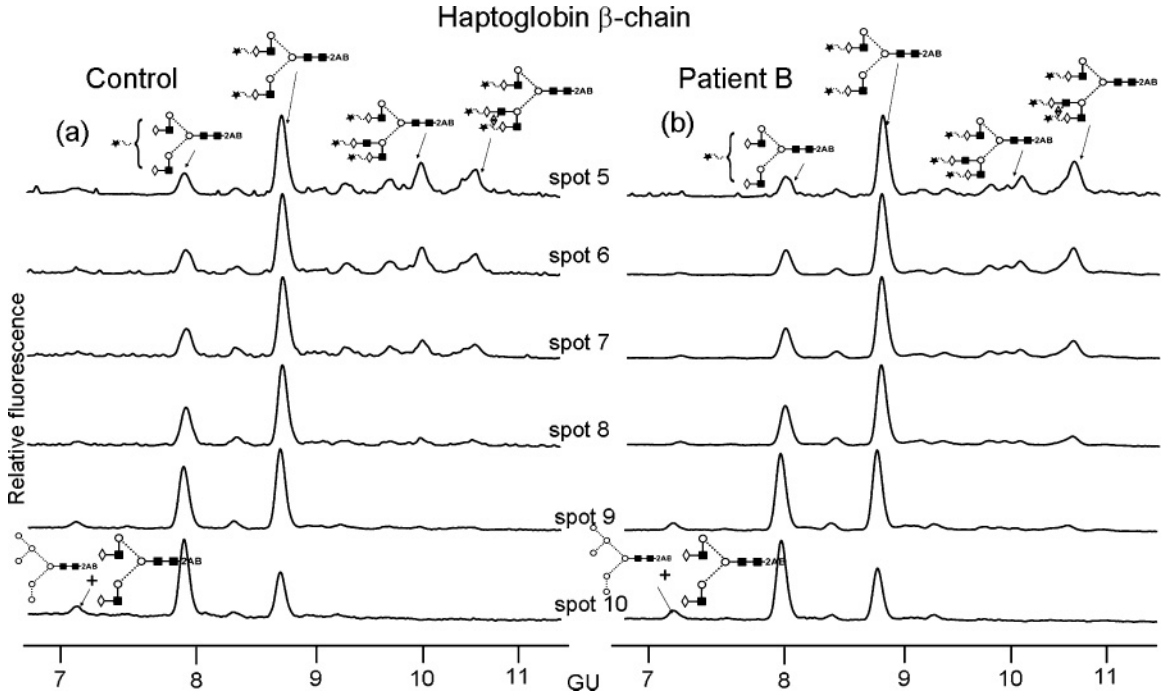

Fig. 6. NPHPLC chromatograms of serum glycans released from haptoglobin β-chain 2D gel spots from (**a**) control and (**b**) patient B (stage III ovarian cancer).

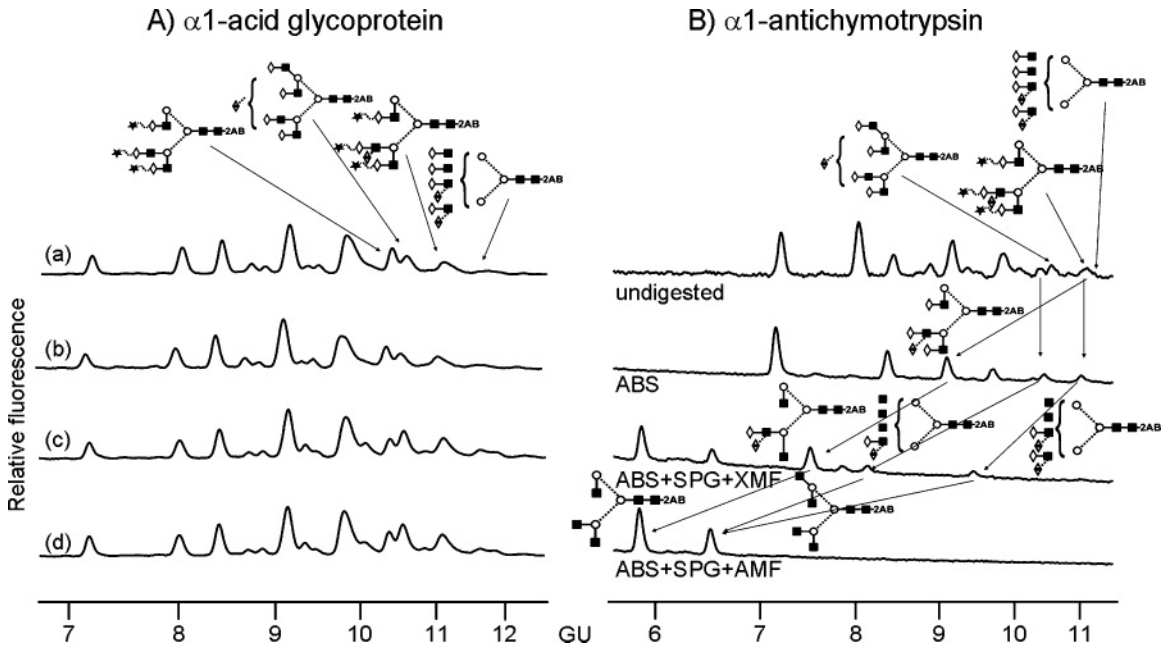

Fig. 7. NPHPLC chromatograms of serum glycans released from (**A**) α1-acid glycoprotein 2D gel spots from pooled (a) control, (b) benign, (c) malignant and (d) metastatic samples and from (**B**) α1-antichymotrypsin from pooled malignant samples excised from 2D gel digested by exoglycosidases for structural assignment of the outer arm fucosylated structures. The exoglycosidases used were: ABS – removes sialic acid, SPG – removes β1,4 linked galactose, XMF – removes α1,2 linked fucose, and AMF – removes α1,3 and α1,4 linked fucose.

levels, which reflect both acute and chronic inflammation, and is currently used for cancer prognosis (MacDonald 2007). The correlation between CRP and SLe^x levels show that there may be some relationship between the mechanisms underlying the CRP response in inflammation and those causing the changes seen in glycosylation in cancer, but they are not identical, as some patients with elevated CRP do not have elevated SLe^x and vice versa. Consistent with this finding, we could not identify any changes in the serum glycome of the malignant melanoma patients (Figure 3) where no inflammation is involved.

In general, in contrast to acute inflammatory conditions, cancers induce chronic inflammation. Monocytes and macrophages infiltrate the tumor to deal with cell debris that forms as a result of necrosis of tumor cells, for example in hypoxia. Macrophages secrete chemotactic factors that enable the recruitment of T cells and this also increases the inflammatory burden. Ovarian tumor cells also secrete cytokines (Huleihel et al. 1997; Nilsson et al. 2005) that can influence glycan processing in both the tumor cells and surrounding tissue (Partridge et al. 2004; Ishibashi et al. 2005). Our data are consistent with the possibility that the tumor process has released factors which alter the glycosylation profile of liver proteins and, importantly, raise the possibility that some of the altered glycoforms of haptoglobin, α1-acid glycoprotein, and α1-antichymotrypsin may be tumor derived. In the case of pancreatic and prostate cancer, RNase 1 and PSA glycoforms, respectively, in patients' sera also appear to be a mixture, derived from both normal healthy processes and from the tumor (Tabares et al. 2006; Barrabes et al. 2007).

Another striking difference in ovarian cancer serum when compared with control serum is the doubling in the levels of FA2. This structure has previously been shown to be attached predominantly to IgG (Parekh et al. 1985; Butler et al. 2003).

Wong et al. described the major *N*-glycans attached to CA125 as mostly monofucosylated biantennary, triantennary, and tetraantennary bisected structures with no more than one sialic acid (Kui Wong et al. 2003). Comparing the CA125 glycans with our major glycan level changes, we propose that elevated levels of CA125 do not contribute to the major changes in whole serum glycans. The glycosylation changes may relate to specific glycoforms of particular glycoproteins in the serum.

Identification of serum glycoproteins containing the altered levels of glycans

Acute-Phase Response The acute-phase response, which occurs during infection, trauma, surgery, burns or inflammatory conditions, leads to substantial changes in the plasma concentration of acute-phase proteins as a result of increased release of inflammatory cytokines such as IL-6 and TNF which stimulate the increased production of CRP, serum amyloid A, haptoglobin, α1-acid glycoprotein, α1-antitrypsin, α1-antichymotrypsin, and fibrinogen (positive acute-phase proteins) along with decreased levels of albumin and transferrin (negative acute-phase proteins). Using our sensitive quantitative techniques in a pilot study, we have identified altered glycosylation on haptoglobin, α1-acid glycoprotein, and α1-antichymotrypsin in advanced ovarian cancer patient sera.

Increase of positive acute-phase proteins in plasma correlates with altered glycosylation

Haptoglobin is a liver protein secreted into plasma which binds free haemoglobin in the plasma and makes it accessible to degradative enzymes. Haptoglobin β-chain expression increases in ovarian cancer, decreases with chemotherapy, and correlates

with CA125 levels (Ahmed et al. 2005). This increase in protein levels could account for some of the changes in the serum glycome. However, our results (Figure 6) from the 2D gel analysis also show an increase in the SLe^x structure on the haptoglobin β-chain. This is consistent with results by Thompson and Turner (1987) who identified an increased fucose content of haptoglobin which increased with tumor size. We have also found the SLe^x structure elevated on α1-acid glycoprotein and α1-antichymotrypsin (Figure 7).

Interestingly, our data suggest that only proteins that normally put on SLe^x have increased levels of this marker. Proteins which do not express SLe^x do not add it in ovarian cancer, e.g., transferrin (unpublished data).

Decreased galactosylation on immunoglobulin G has impact on its function

Our *N*-linked analysis of the glycans on IgG from the ovarian cancer patients showed a trend toward decreasing levels of galactosylation and sialylation (Figure 4 and Table IV). An increase of agalactosyl IgG oligosaccharides can be the result of decreased Gal-T activity in plasma cells (Axford et al. 1992), or increased production of specific subsets of plasma cells with low expression levels of galactosyltransferases (Omtvedt et al. 2006). Different glycoforms may differ in efficiency of interaction with ligands (Malhotra et al. 1995; Umana et al. 1999; Shields et al. 2002; Kaneko et al. 2006). The IgG-G0 glycoform is elevated in rheumatoid arthritis serum (Parekh et al. 1985) and terminal GlcNAc of this glycoform on the Fc region of the IgG molecule clustered, for example on synovial tissue, can be recognized by the serum lectin mannose-binding protein (MBL) resulting in complement activation (Malhotra et al. 1995). Kaneko et al. (2006) has shown that sialylation of IgG reduces cytotoxicity of natural killer cells, exhibiting an anti-inflammatory effect. Increase of the agalactosyl IgG glycoform has predominantly been identified with tumor progression and metastasis of gastric and lung cancer (Kanoh et al. 2004), as well as in other diseases such as rheumatoid arthritis, tuberculosis, inflammatory bowel disease (Parekh et al. 1985; Axford et al. 1992), and vasculitis (Holland et al. 2002).

Summary

In conclusion, our newly developed high-throughput techniques enabled us to monitor glycosylation changes in whole serum rapidly. We have described differences between control and advanced ovarian cancer sera: a doubling in the amount of FA2 and SLe^x structures in whole serum glycan profiles and a shift in the sialic acid linkage from α2,3 to α2,6 in disialylated fractions. We have demonstrated that the level of SLe^x alone is not specific for ovarian cancer, but a combination of FA2 and SLe^x significantly improves the separation of benign gynecological conditions from ovarian cancer. To investigate further which protein glycans contribute to these changes in total serum glycans, we focused on the inflammatory system identifying serum glycoproteins carrying these glycans. Our newly developed sensitive HPLC-based technology enabled us to screen the selected proteins simultaneously from the same patient. This analysis of the glycosylation of protein excised from single spots on a 2D minigel show: haptoglobin β-chain, α1-acid glycoprotein, and α1-antichymotrypsin with elevated SLe^x structure and IgG with decreased galactosylation and sialylation. Only proteins containing SLe^x in controls have increased levels of this epitope in patients. This preliminary investigation exploring phenomenological changes in ovarian cancer patients provides some insight into the pathogenesis, and suggests that more extensive studies of clusters of related proteins and the serum glycome may lead to potential biomarkers.

Materials and methods

Serum samples

Venous blood samples were obtained from (a) healthy controls and patients undergoing treatment at St. James's University Hospital (Leeds, UK) and (b) from healthy donors and melanoma patients participating in a research program of the Institute of Biochemistry (Bucharest, Romania), following ethical approval and obtaining informed consent. After allowing the blood to clot for 30–60 min, serum was obtained by centrifugation at 2000 × *g* for 10 min and stored at −80°C until analysis.

(a) For the initial pilot study, samples from three patients with ovarian cancer were used (patient A, stage IIIC serous and endometrioid carcinoma prior to surgery; patients B and C, stage III serous carcinoma at the time of relapse with advanced disease; age range 60–72 years) and compared with a serum pool formed from five females of similar age). For the screening of serum proteins carrying glycosylation changes pooled control serum formed from eight females of similar age was compared to pooled serum formed from three females with benign gynecological conditions (principally serous adenoma or cysts); malignant ovarian cancer (one serous and endometrioid carcinoma, one bilateral serous adenocarcinoma, and one bilateral papillary adenocarcinoma); and metastatic ovarian cancer (two papillary serous adenocarcinoma, one serous carcinoma).

For the main part of the study, samples from a further 90 controls and patients with ovarian cancer, other gynecological cancers, or benign gynecological conditions were used (Table III). Serum concentrations of CRP were analysed using an Advia 1650 analyzer (Bayer, Newbury, UK) and CA125 using a Centaur analyzer (Bayer). Reference ranges were <10 mg/L and <35 U/mL.

(b) For the study, following patients with malignant melanoma have been used to compare with three healthy controls (age range 35–52 years): four patients with malignant melanoma, pigmented, invasion Clark-3 to Clark-4 (three nonulcerated, one ulcerated, age range 30–58 years), one patient 6 months from surgery for a malignant melanoma tumor, posterior chest (36 years old), one patient with abdominal dysplastic nevus, 0.8 mm/0.2 mm diameter (47 years old), and one patient with hyperpigmented malignant melanoma tumors, located on anterior chest and underclavicula (52 years old). This patient had as previous tumor and underwent surgery and chemotherapy. Fibrinogen was determined as clottable protein using the method described by Swaim and Feders (1967). Reference ranges were 200–400 ng/mL.

Release and purification of N*-glycans from human serum in gel block*

N-Glycans were released from glycoproteins in serum samples by in situ digestion with *N*-glycosidase F (PNGase F, Roche, Mannheim, Germany) (a) in SDS-PAGE gel bands as described

earlier (Royle et al. 2006) or (b) in-gel blocks as described by (Royle et al. 2006). Briefly, serum samples were reduced and alkylated, then set into SDS-gel blocks, washed and *N*-glycan released by PNGase F.

Fluorescent labeling of the reducing terminus of N-*glycans*

Glycans were fluorescently labeled with 2-aminobenzamide (2AB) by reductive amination (Bigge et al. 1995) (LudgerTag 2-AB labeling kit LudgerLtd., Abingdon, UK).

Exoglycosidase digestion of 2AB labeled N-*linked glycans*

All enzymes were purchased from Glyko (Novato, CA) or New England Biolabs (Hitchin, Herts, UK). The 2AB-labeled glycans were digested in a volume of 10 μL for 18 h at 37°C in 50 mM sodium acetate buffer, pH 5.5 (except in the case of jack bean α-mannosidase (JBM) where the buffer was 100 mM sodium acetate, 2 mM Zn^{2+}, pH 5.0), using arrays of the following enzymes: ABS – *Arthrobacter ureafaciens* sialidase (EC 3.2.1.18), 1 U/mL; NAN1-Streptococcus pneumoniae sialidase (EC 3.2.1.18), 1 U/mL; BTG – bovine testes β-galactosidase (EC 3.2.1.23), 1 U/mL; SPG – *S. pneumoniae* β-galactosidase (EC 3.2.1.23), 0.1 U/mL; BKF – bovine kidney alpha-fucosidase (EC 3.2.1.51), 1 U/mL; GUH – β-*N*-acetylglucosaminidase cloned from *S. pneumonia,* expressed in *Escherichia. coli* (EC 3.2.1.30), 4 U/mL; JBM (EC 3.2.1.24) , 50 U/mL; AMF – almond meal alpha-fucosidase (EC 3.2.1.111), 3 mU/ mL, XMF – *Xanthomonus* sp. alpha-fucosidase (EC 3.2.1.51.), 0.1 U/mL.

After incubation, enzymes were removed by filtration through a protein-binding EZ filters (Millipore Corporation, Beford, MA) (Royle et al. 2006), the *N*-glycans were then analyzed by NP-HPLC and WAX-HPLC.

HPLC

NP-HPLC was performed using a TSK-Gel Amide-80 4.6 × 250 mm column (Anachem, Luton, UK) on a 2695 Alliance separations module (Waters, Milford, MA) equipped with a Waters temperature control module and a Waters 2475 fluorescence detector. Solvent A was 50 mM formic acid adjusted to pH 4.4 with ammonia solution. Solvent B was acetonitrile. The column temperature was set to 30°C. Gradient conditions were a linear gradient of 26–52% A, over 104 min at a flow rate of 0.4 mL/min. Samples were injected in 74% acetonitrile (Royle et al. 2006). Fluorescence was measured at 420 nm with excitation at 330 nm. The system was calibrated using an external standard of hydrolyzed and 2AB-labeled glucose oligomers to create a dextran ladder, as described previously (Royle et al. 2006).

WAXHPLC was performed using a Vydac 301VHP575 7.5 × 50 mm column (Anachem, Luton, Bedfordshire, UK) as described (Royle et al. 2006). Briefly, solvent A was 0.5 M ammonium formate, pH 9. Solvent B was 10% (v/v) methanol in water. Gradient conditions were a linear gradient of 0–5% A over 12 min at a flow rate of 1 mL/min, followed by 5–21% A over 13 min, then 21–50% A over 25 min, 80–100% A over 5 min, then 5 min at 100% A. Samples were injected in water.

MALDI-TOF MS

Positive ion MALDI-TOF mass spectra were recorded with a Micromass TofSpec 2E reflectron-TOF mass spectrometer (Micromass, Manchester, UK) fitted with delayed extraction and a nitrogen laser (337 nm). The acceleration voltage was 20 kV; the pulse voltage was 3200 V; the delay for the delayed extraction ion source was 500 ns. Samples were prepared by adding 0.5 mL of an aqueous solution of the sample to the matrix solution (0.3 mL of a saturated solution of 2,5-dihydroxybenzoic acid in acetonitrile) on the stainless steel target plate and allowing it to dry at room temperature (RT). The sample/matrix mixture was then recrystallized from ethanol (Harvey 1993).

Negative ion electrospray ionization mass spectrometry (ESI-MS) and ESI MS/MS

Nanoelectrospray mass spectrometry was performed with a Waters–Micromass quadrupole (Q)-TOF Ultima Global instrument. Samples in 1:1 (v:v) methanol:water containing 0.5 mM ammonium phosphate were infused through Proxeon (Proxeon Biosystems, Odense, Denmark) nanospray capillaries. The ion source conditions were: temperature, 120°C; nitrogen flow, 50 L/h; infusion needle potential, 1.2 kV; cone voltage, 100 V; RF-1 voltage, 180 V. Spectra (2 s scans) were acquired with a digitization rate of 4 GHz and accumulated until a satisfactory signal:noise ratio had been obtained. For MS/MS data acquisition, the parent ion was selected at low resolution (about 4*m*/*z* mass window) to allow transmission of isotope peaks and fragmented with argon. The voltage on the collision cell was adjusted with mass and charge to give an even distribution of fragment ions across the mass scale. Typical values were 80–120 V.

Purification of serum IgG

Serum (5 μL) was diluted 100-fold with 0.1 M Tris, 1 M NaCl, 1 mM EDTA, pH 7.5 and applied to a Protein G column (Pharmacia Biotech, Uppsala, Sweden). The column was equilibrated and washed with 15 mL of 0.1 M Tris, 1 M NaCl, 1 mM EDTA, pH 7.5, and the IgG was eluted with 0.1 M glycine–HCl, pH 2.7 into 1.5 mL tubes containing 100 μL 0.1 M Tris, 1 M NaCl, 1 mM EDTA buffer (pH 7.5). The fractions containing IgG were pooled and dialyzed against 1 × PBS overnight at 4°C using a dialysis membrane (Medicell International Ltd., London, UK). The dialyzed IgG was concentrated by adding 10 μl resin (Strata clean resin, Stratagene, La Jolla, CA) and left at RT for 1 h at slow rotation for binding. After centrifugation at 1000 × *g*, the supernatant was removed to leave about 10 μL of pellet in the bottom of the tube, this was reduced and alkylated and transferred to SDS-PAGE gel. Following electrophoresis, the pure IgG heavy chain band was cut out from the gel for glycan analysis.

Electrophoresis

Electrophoresis in 4–12% Bis-Tris SDS-PAGE mini-gels (Invitrogen, Carlsbad, CA) was performed at RT according to the method of Laemmli (1970). The gels were Coomassie stained. All samples were reduced with 5% 2-mercaptoethanol before analysis. Approximately 40 μg of proteins from sera was loaded per lane.

2-Dimensional electrophoresis (2-DE)

Eighty micrograms of the human serum were dissolved in 120 μL of sample buffer (5 M urea, 2 M thiourea, 2 mM tributyl-phosphine, 65 mM dithiothreitol (DTT), 4% 3-[(3- cholamidopropyl) dimethylammonio]- 1 - propanesulfonate (CHAPS), 4% v/w NDSB-256, trace of bromophenol blue) and

subjected to 2-DE. Ampholytes were added to the sample at 0.9% Servalyte 3–10, 0.45% Servalyte 2–4 and 9–11. Immobilized pH gradient gels (Immobiline DryStrip 3–10 NL, 7 cm) were rehydrated in the sample and isoelectric focusing (IEF) was carried out according to the method described by Sanchez (Sanchez et al. 1997) at 17°C but with modified voltages and times as following: first minute 200 V, 3 mA, 5 W, then 3500 V, 3 h and 30 min, 10 mA, 5 W. Following focusing, the immobilized pH gradient (IPG) strips were immediately equilibrated for 15 min in 4 M urea, 2 M thiourea, 2% (w/v) DTT, 30% glycerol, 50 mM Tris, pH 6.8, 2% SDS, trace of bromophenol blue. Proteins were separated in the second dimension at 125 V for 2 h at RT, on 4–12% Bis–Tris gradient gels (Invitrogen). Following electrophoresis, the gels were fixed in 40% (v/v) ethanol: 10% (v/v) acetic acid and stained with the fluorescent dye OGT 1238 (Oxford Glycosciences, Abingdon, UK) according to the method described previously (Hassner et al. 1984). Monochrome fluorescence images were obtained by scanning gels with an Apollo II linear fluorescent scanner (Oxford Glycosciences).

Glycan analysis of 2-DE gel spots

Glycans were released and extracted from the 1 mm^3 of gel excised for MS analysis. The procedure used was the in-gel block method for human serum described earlier (Royle et al. 2006), with modifications. The gel pieces were frozen for >2 h, and then washed for 15 min with shaking with alternating 1 mL acetonitrile and 1 mL 20 mM $NaHCO_3$ for three washes. After each step the washings were removed under vacuum. The glycoproteins were not reduced and alkylated before loading on the gel; therefore, reduction and alkylation were carried out in situ: the gel pieces were incubated at 37°C for 30 min with 20 μL 0.5 M DTT plus 180 μl 20 mM $NaHCO_3$, then 20 μL 100 mM IAA were added and incubation continued for further 30 min at RT. The procedure then followed the in-gel block method starting with five alternating washes with acetonitrile and 20 mM $NaHCO_3$. Sufficient PNGaseF was added to cover the gel pieces. Released glycans were eluted with three washes with 200 μL water and another three alternating washes with 200 μL acetonitrile and 200 μL water, each wash for 30 min, formic acid treated and labeled with the fluorophore 2AB as described earlier (Bigge et al. 1995; Royle et al. 2006). Sufficient glycans were produced by these procedures for up to 10 NP-HPLC chromatograms, including digestions. The proteins which remained in the gel spots were identified by MS.

Identification of proteins in gel spots from 2-DE (see Table V) by mass spectrometric analysis

Mass spectrometric analysis was carried out using a Q-TOF 1 (Micromass, Manchester, UK) coupled to a CapLC (Waters). Tryptic peptides were concentrated and desalted on a 300 μm id/5 mm C18 precolumn and resolved on a 75 μm id/25 cm C18 PepMap analytical column (LC packings, SanFrancisco, CA). Peptides were eluted to the mass spectrometer using a 45 min 5–95% acetonitrile gradient containing 0.1% formic acid at a flow rate of 200 nL/min. Spectra were acquired in a positive mode with a cone voltage of 40 V and a capillary voltage of 3300 V. The MS to MS/MS switching was controlled in an automatic-data-dependent fashion with a 1-s survey scan followed by three 1-s MS/MS scans of the most intense ions. Precursor ions selected for MS/MS were excluded from further fragmentation for 2 min. Spectra were processed using ProteinLynx Global server 2.1.5 and searched against the SWISS-PROT and NCBI databases using the MASCOT search engine (Matrix Science, London, UK). Searches were restricted to the human taxonomy allowing carbamidomethyl cysteine as a fixed modification and oxidized methionine as a potential variable modifications. Data were searched allowing 0.5 Da error on all spectra and up to two missed tryptic cleavage sites to accommodate calibration drift and incomplete digestion, all data were checked for consistent error distribution.

Statistical analysis

Nonparametric statistical tests were used with Kruskal–Wallis test for the comparison of all groups for SLe^x levels and subsequent Mann–Whitney tests for the comparison of individual groups. Correlation analysis was carried out using two-tailed Spearman test. In all cases, a $p < 0.05$ was taken as the cutoff level for significance.

Funding

This study was supported by the Oxford Glycobiology Institute endowment fund and EUROCarbDB (http://www.eurocarbdb.org) RIDS Contract No. 011952. The Biotechnology and Biological Sciences Research Council and the Wellcome Trust provided equipment grants to purchase the Waters-Micromass TofSpec 2E and the Q-Tof mass spectrometers, respectively.

Acknowledgements

We would like to thank to all the members of Prof. Pauline Rudd's group for technical help and support, the sample technicians within the Cancer Research UK Clinical Centre at Leeds for help with sample collection, and Dr. Margaret Huflejt for useful discussions.

Conflict of interest statement

None declared.

Abbreviations

2AB, 2-aminobenzamide; ABS, *Arthrobacter ureafaciens* sialidase; AMF, almond meal alpha-fucosidase; BKF, bovine kidney alpha-fucosidase; BTG, bovine testes β-galactosidase; CHAPS, 3-[(3-cholamidopropyl)dimethylammonio]-1-propanesulfonate; CRP, C-reactive protein; 2-DE, 2-dimensional electrophoresis; DTT, dithiothreitol; GU, glucose units; GUH, β-*N*-acetylglucosaminidase cloned from *Streptococcus pneumonia,* expressed in *Escherichia coli*; HPLC, high-performance liquid chromatography; IAA, iodoacetic acid; IEF, isoelectric focusing; IPG, immobilized pH gradient; JBM, jack bean α-mannosidase; MALDI, matrix-assisted laser desorption/ionization; MS, mass spectrometry; NAN1, *Streptococcus pneumoniae* sialidase; NP, normal phase; PAGE, polyacrylamide gel electrophoresis; PPC, primary peritoneal

carcinomatosis; RT, room temperature; SDS, sodium dodecyl sulphate; SLe^x, sialyl Lewis x; SPG, *Streptococcus pneumoniae* β-galactosidase; TOF, time-of-flight; WAX, weak anion exchange; XMF, *Xanthomonus* sp. alpha-fucosidase.

References

Ahmed N, Oliva KT, Barker G, Hoffmann P, Reeve S, Smith IA, Quinn Rice MA, GE. 2005. Proteomic tracking of serum protein isoforms as screening biomarkers of ovarian cancer. Proteomics. 5:4625–4636.

Aubert M, Panicot L, Crotte C, Gibier P, Lombardo D, Sadoulet MSO, Mas E. 2000. Restoration of alpha(1,2) fucosyltransferase activity decreases adhesive and metastatic properties of human pancreatic cancer cells. Cancer Res. 60:1449–1456.

Aubert M, Panicot-Dubois L, Crotte C, Sbarra V, Lombardo D, Sadoulet MO, Mas E. 2000. Peritoneal colonization by human pancreatic cancer cells is inhibited by antisense FUT3 sequence. Int J Cancer. 88:558–565.

Axford JS, Sumar N, Alavi A, Isenberg DA, Young A, Bodman KB, Roitt IM. 1992. Changes in normal glycosylation mechanisms in autoimmune rheumatic disease. J Clin Invest. 89:1021–1031.

Barrabes S, Pages-Pons L, Radcliffe CM, Tabares G, Fort E, Royle L, Harvey DJ, Moenner M, Dwek RA, Rudd PM, et al. 2007. Glycosylation of serum ribonuclease 1 indicates a major endothelial origin and reveals an increase in core fucosylation in pancreatic cancer. Glycobiology. 17:388–400.

Bast RC Jr., Badgwell D, Lu Z, Marquez R, Rosen D, Liu J, Baggerly KA, Atkinson EN, Skates S, Zhang Z, et al. 2005. New tumor markers: CA125 and beyond. Int J Gynecol Cancer. 15(Suppl 3):274–281.

Bengtsson S, Krogh M, Szigyarto CA, Uhlen M, Schedvins K, Silfversward C, Linder S, Auer G, Alaiya A, James P. 2007. Large-scale proteomics analysis of human ovarian cancer for biomarkers. J Proteome Res. 6:1440–1450.

Bigge JC, Patel TP, Bruce JA, Goulding PN, Charles SM, Parekh RB. 1995. Nonselective and efficient fluorescent labeling of glycans using 2-amino benzamide and anthranilic acid. Anal Biochem. 230:229–238.

Brinkman-van der Linden EC, de Haan PF, Havenaar EC, van Dijk W. 1998. Inflammation-induced expression of sialyl LewisX is not restricted to alpha1-acid glycoprotein but also occurs to a lesser extent on alpha1-antichymotrypsin and haptoglobin. Glycoconj J. 15:177–182.

Butler M, Quelhas D, Critchley AJ, Carchon H, Hebestreit HF, Hibbert RG, Vilarinho L, Teles E, Matthijs G, Schollen E, et al. 2003. Detailed glycan analysis of serum glycoproteins of patients with congenital disorders of glycosylation indicates the specific defective glycan processing step and provides an insight into pathogenesis. Glycobiology. 13:601–622.

Crispin MD, Ritchie GE, Critchley AJ, Morgan BP, Wilson IA, Dwek RA, Sim RB and Rudd PM. 2004. Monoglucosylated glycans in the secreted human complement component C3: implications for protein biosynthesis and structure. FEBS Lett. 566:270–274.

De Graaf TW, Van der Stelt ME, Anbergen MG, van Dijk W. 1993. Inflammation-induced expression of sialyl Lewis X-containing glycan structures on alpha 1-acid glycoprotein (orosomucoid) in human sera. J Exp Med. 177:657–666.

Dube DH and Bertozzi CR. 2005. Glycans in cancer and inflammation–potential for therapeutics and diagnostics. Nat Rev Drug Discov. 4:477–488.

Duffy MJ, Bonfrer JM, Kulpa J, Rustin GJ, Soletormos G, Torre GC, Tuxen MK, Zwirner M. 2005. CA125 in ovarian cancer: European Group on Tumor Markers guidelines for clinical use. Int J Gynecol Cancer. 15:679–691.

Fukuda M, Spooncer E, Oates JE, Dell A, Klock JC. 1984. Structure of sialylated fucosyl lactosaminoglycan isolated from human granulocytes. J Biol Chem. 259:10925–10935.

Gercel-Taylor C, Bazzett LB and Taylor DD. 2001. Presence of aberrant tumor-reactive immunoglobulins in the circulation of patients with ovarian cancer. Gynecol Oncol. 81:71–76.

Harvey DJ. 1993. Quantitative aspects of the matrix-assisted laser desorption mass spectrometry of complex oligosaccharides. Rapid Commun Mass Spectrom. 7:614–619.

Harvey DJ. 2005a. Fragmentation of negative ions from carbohydrates: part 1. Use of nitrate and other anionic adducts for the production of negative ion electrospray spectra from N-linked carbohydrates. J Am Soc Mass Spectrom. 16:622–630.

Harvey DJ. 2005b. Fragmentation of negative ions from carbohydrates: part 2. Fragmentation of high-mannose N-linked glycans. J Am Soc Mass Spectrom. 16:631–646.

Harvey DJ. 2005c. Fragmentation of negative ions from carbohydrates: part 3. Fragmentation of hybrid and complex N-linked glycans. J Am Soc Mass Spectrom. 16: 647–659.

Hassner A, Birnbaum D and Loew LM. 1984. Charge-shift probes of membrane potential. Synthesis. J Org Chem. 49:2546–2551.

He Z, Aristoteli LP, Kritharides L and Garner B. 2006. HPLC analysis of discrete haptoglobin isoform N-linked oligosaccharides following 2D-PAGE isolation. Biochem Biophys Res Commun. 343:496–503.

Holland M, Takada K, Okumoto T, Takahashi N, Kato K, Adu D, Ben-Smith A, Harper L, Savage CO, Jefferis R. 2002. Hypogalactosylation of serum IgG in patients with ANCA-associated systemic vasculitis. Clin Exp Immunol. 129:183–190.

Huleihel M, Maymon E, Piura B, Prinsloo I, Benharroch D, Yanai-Inbar I, Glezerman M. 1997. Distinct patterns of expression of interleukin-1 alpha and beta by normal and cancerous human ovarian tissues. Eur Cytokine Netw. 8:179–187.

Ishibashi Y, Inouye Y, Okano T, Taniguchi A. 2005. Regulation of sialyl-Lewis x epitope expression by TNF-alpha and EGF in an airway carcinoma cell line. Glycoconj J. 22:53–62.

Kaneko Y, Nimmerjahn F, Ravetch JV. 2006. Anti-inflammatory activity of immunoglobulin G resulting from Fc sialylation. Science. 313:670–673.

Kanoh Y, Mashiko T, Danbara M, Takayama Y, Ohtani S, Imasaki T, Abe T and Akahoshi T. 2004. Analysis of the oligosaccharide chain of human serum immunoglobulin g in patients with localized or metastatic cancer. Oncology. 66:365–370.

Kim YJ, Varki A. 1997. Perspectives on the significance of altered glycosylation of glycoproteins in cancer. Glycoconj J. 14:569–576.

Kozak KR, Su F, Whitelegge JP, Faull K, Reddy S, Farias-Eisner R. 2005. Characterization of serum biomarkers for detection of early stage ovarian cancer. Proteomics. 5:4589–4596.

Kui Wong N, Easton RL, Panico M, Sutton-Smith M, Morrison JC, Lattanzio FA, Morris HR, Clark GF, Dell A, Patankar MS. 2003. Characterization of the oligosaccharides associated with the human ovarian tumor marker CA125. J Biol Chem. 278:28619–28634.

Laemmli UK. 1970. Cleavage of structural proteins during the assembly of the head of bacteriophage T4. Nature. 227:680–685.

Llorca J, Lopez-Diaz MJ, Gonzalez-Juanatey C, Ollier WE, Martin J, Gonzalez-Gay MA. 2007. Persistent chronic inflammation contributes to the development of cancer in patients with rheumatoid arthritis from a defined population of northwestern Spain. Semin Arthritis Rheum. 37:31–38.

MacDonald N. 2007. Cancer cachexia and targeting chronic inflammation: a unified approach to cancer treatment and palliative/supportive care. J Support Oncol. 5:157–162; discussion 164–156, 183.

Magnani JL. 2004. The discovery, biology. and drug development of sialyl Lea and sialyl Lex. Arch Biochem Biophys. 426:122–131.

Malhotra R, Wormald MR, Rudd PM, Fischer PB, Dwek RA, Sim RB. 1995. Glycosylation changes of IgG associated with rheumatoid arthritis can activate complement via the mannose-binding protein. Nat Med. 1:237–243.

McEver RP. 1997. Selectin-carbohydrate interactions during inflammation and metastasis. Glycoconj J. 14:585–591.

Nilsson MB, Langley RR, Fidler IJ. 2005. Interleukin-6, secreted by human ovarian carcinoma cells, is a potent proangiogenic cytokine. Cancer Res. 65:10794–10800.

Omtvedt LA, Royle L, Husby G, Sletten K, Radcliffe CM, Harvey DJ, Dwek RA, Rudd PM. 2006. Glycan analysis of monoclonal antibodies secreted in deposition disorders indicates that subsets of plasma cells differentially process IgG glycans. Arthritis Rheum. 54:3433–3440.

Parekh RB, Dwek RA, Sutton BJ, Fernandes DL, Leung A, Stanworth D, Rademacher TW, Mizuochi T, Taniguchi T, Matsuta K, et al. 1985. Association of rheumatoid arthritis and primary osteoarthritis with changes in the glycosylation pattern of total serum IgG. Nature. 316:452–457.

Partridge EA, Le Roy C, Di Guglielmo GM, Pawling J, Cheung P, Granovsky M, Nabi IR, Wrana JL, Dennis JW. 2004. Regulation of cytokine receptors by golgi *N*-glycan processing and endocytosis. Science. 306:120–24.

Royle L, Radcliffe CM, Dwek RA, Rudd PM. 2006. Detailed structural analysis of *N*-glycans released from glycoproteins in SDS-PAGE gel bands using HPLC combined with exoglycosidase array digestions. Methods Mol Biol. 347:125–143.

Sanchez JC, Rouge V, Pisteur M, Ravier F, Tonella L, Moosmayer M, Wilkins MR, Hochstrasser DF. 1997. Improved and simplified in-gel sample application using reswelling of dry immobilized pH gradients. Electrophoresis. 18:324–327.

Shields RL, Lai J, Keck R, O'Connell LY, Hong K, Meng YG, Weikert SH, Presta LG. 2002. Lack of fucose on human IgG1 N-linked oligosaccharide improves binding to human Fcgamma RIII and antibody-dependent cellular toxicity. J Biol Chem. 277:26733–26740.

Swaim WR and Feders MB. 1967. Fibrinogen assay. Clin Chem. 13:1026–1028.

Tabares G, Radcliffe CM, Barrabes S, Ramirez M, Aleixandre RN, Hoesel W, Dwek RA, Rudd PM, Peracaula R, de Llorens R. 2006. Different glycan structures in prostate-specific antigen from prostate cancer sera in relation to seminal plasma PSA. Glycobiology. 16:132–145.

Thompson S and Turner GA. 1987. Elevated levels of abnormally-fucosylated haptoglobins in cancer sera. Br J Cancer. 56:605–610.

Turner GA, Goodarzi MT, Thompson S. 1995. Glycosylation of alpha-1-proteinase inhibitor and haptoglobin in ovarian cancer: evidence for two different mechanisms. Glycoconj J. 12:211–218.

Umana P, Jean-Mairet J, Moudry R, Amstutz H, Bailey JE. 1999. Engineered glycoforms of an antineuroblastoma IgG1 with optimized antibody-dependent cellular cytotoxic activity. Nat Biotechnol. 17:176–180.

Wang PH, Lee WL, Juang CM, Yang YH, Lo WH, Lai CR, Hsieh SL, Yuan CC. 2005. Altered mRNA expressions of sialyltransferases in ovarian cancers. Gynecol Oncol. 99:631–639.

Ye B, Skates S, Mok SC, Horick NK, Rosenberg HF, Vitonis A, Edwards D, Sluss P, Han WK, Berkowitz RS, et al. 2006. Proteomic-based discovery and characterization of glycosylated eosinophil-derived neurotoxin and COOH-terminal osteopontin fragments for ovarian cancer in urine. Clin Cancer Res. 12:432–441.